An Isotropic Electric-Field Probe with Tapered Resistive Dipoles for Broad-Band Use, 100 kHz to 18 GHz

MOTOHISA KANDA, SENIOR MEMBER, IEEE, AND LANNY D. DRIVER

Abstract—**A new broad-band electric-field probe, capable of accurately characterizing and quantifying electromagnetic (EM) fields, has been developed at the National Bureau of Standards (NBS). The probe's 8-mm resistively tapered dipole elements allow measurement of electric fields between 1 and 1600 V/m from 1 MHz to 15 GHz, with a flatness of ±2 dB. A mutually orthogonal dipole configuration provides an overall standard deviation in isotropic response, with respect to angle, that is within ±0.3 dB. Both the theoretical and developmental aspects of this prototype electric-field probe are discussed in this paper.**

I. Introduction

THE EVER-EXPANDING spectrum of applications involving standard electromagnetic (EM) fields has resulted in a corresponding growing need for improved and expanded EM field testing facilities, equipment, and techniques. Anechoic chambers, transverse electromagnetic mode (TEM) cells, and open-field ranges are finding increasing usage for establishing standard, well-characterized EM fields. A growing interest in hazard assessments of nonionizing electromagnetic emissions from electronic equipment on biological or simulated tissue has created a need for improved EM field measurements in both free space and material mediums. Central to all these requirements lies a need for EM field sensing devices with higher frequency, broader bandwidth, smaller size, and higher accuracy.

Establishing standards for EM field measurements is a multifaceted endeavor which requires 1) the generation of standard EM fields and 2) the capability of performing rigorous EM measurements using transfer-standard probes. Standard EM fields are typically required at open-field sites, in TEM cells, in guided-wave structures, and in anechoic chambers. The requirements for establishing standard EM fields have been previously reported [1], [2]. This paper addresses the many developmental aspects of producing a transfer-standard probe having a known response over wide ranges of frequency and amplitude.

The National Bureau of Standards (NBS) is currently engaged in an ongoing effort to design and develop improved broad-band electric-field (*E*-field) probes [3]. This work has recently produced a new prototype transfer-standard *E*-field probe that offers a number of significant improvements over conventional *E*-field probes. The probe features 1) an ultrawide useful frequency range of 100 kHz–18 GHz; 2) a frequency response flat to within ±2 dB from 1 MHz to 15 GHz; 3) a wide dynamic measurement range covering 1 to 1600 V/m; 4) an isotropic response whose standard deviation (with respect to angle) is within ±0.3 dB; 5) a small probe body which is only 1 cm in diameter and 4 cm long; and 6) a high-resistance transmission cable for connecting the probe's outputs to an external metering unit.

The heart of the broad-band *E*-field probe consists of three mutually orthogonal, electrically short dipoles, each on its own substrate. The extended flat frequency response of the probe, beyond any natural resonant frequency, is obtained through the use of dipole resistive tapering. A low-barrier, beam-lead Schottky detector diode shunts each dipole's center gap, thereby providing detection of field-induced voltages. Pairs of high-resistance, thin-film leads transmit the detected signals from the dipole–diode combinations to output bonding pads. This paper discusses the theoretical and experimental aspects of the design, fabrication, evaluation, calibration, and application of this broad-band, isotropic *E*-field probe.

II. Design Considerations for a Broad-Band Electric-Field Probe

A. The Resistively Tapered Dipole Element

It is well known that a conventional dipole antenna, which essentially supports a standing-wave current distribution, is highly frequency sensitive [4]. This is a consequence of dipole antenna characteristics such as current distribution, antenna admittance, and radiation pattern being strong functions of frequency. Therefore, the useful frequency range of a conventional metal dipole is usually limited by its natural resonant frequency, which is a direct function of its length. To develop a transfer-standard electric-field probe whose frequency response is relatively flat to *Ku*-band (18 GHz), the length of a conventional metal dipole must be shortened to about 2 to 3 mm. Probes with dipole lengths of 2 to 3 mm, and even submillimeter dimensions, have been developed at the expense of significantly reduced sensitivity and seriously degraded antenna reception characteristics [5].

Manuscript received May 19, 1986; revised September 25, 1986.

The authors are with the Electromagnetic Fields Division, National Bureau of Standards, Boulder, CO 80303.

IEEE Log Number 8611632.

As a means of overcoming the severe size limitations imposed by natural dipole resonance, NBS has demonstrated that a traveling-wave dipole antenna can be realized by continuous resistive tapering of the dipole halves. Detailed studies of the characteristics of resistively tapered dipoles have been extensively pursued by the author [6] and other researchers [7]. Basically, it has been shown that if the internal impedance per unit length $Z^i(z)$ as a function of the axial coordinate z can be expressed as

$$Z^i(z) = \frac{60\psi}{h - |z|} \tag{1}$$

then the current distribution $I_z(z)$ along the linear antenna is that of a traveling wave, i.e.,

$$I_z(z) = \frac{V_0}{60\psi(1 - j/kh)}\left[1 - \frac{|z|}{h}\right]e^{-jk|z|}. \tag{2}$$

The symbols have the following meanings: $2h$ is the dipole's total physical length, k is the wavenumber, V_0 is the driving voltage, and ψ is given by

$$\psi \cong 2\left[\sinh^{-1}\frac{h}{a} - C(2ka,2kh) - jS(2ka,2kh)\right] + \frac{j}{kh}(1 - e^{-j2kh}) \tag{3}$$

where a is the radius of the dipole, and $C(x, y)$ and $S(x, y)$ are the generalized cosine and sine integrals, respectively.

In the present study of developing a broad-band electric-field probe for use in the frequency range between 100 kHz and 18 GHz, an 8-mm-long dipole was selected for optimizing the sensitivity and bandwidth of the antenna, while maintaining a reasonably small physical size. The internal impedance per unit length required to achieve a traveling-wave antenna is given by (1), and can be specifically expressed as

$$Z_l = \frac{60 \times 6.34}{4 - l}\ \Omega/\text{mm} \qquad \text{for} \quad 0 \leqslant l \leqslant 4\ \text{mm} \tag{4}$$

for each side of the dipole. Ideally, the required resistive tapering is 95 Ω/mm at the midpoint ($l = 0$ mm) and infinite at the end of the antenna ($l = 4$ mm). To realize such a resistive tapering profile, the antenna is fabricated by photoetching a thin film of tantalum nitride (TaN), which has a resistivity of 9.5 Ω/sq. Each half of the dipole is 4 mm long and varies linearly in width from 0.15 mm at the dipole gap to 0 mm at the dipole tips, as shown in Fig. 1. This surface resistance and antenna geometry result in the required tapered resistive profile, as illustrated in Fig. 2 and as expressed in (4). Each of the probe's three 8-mm dipole elements, their associated high-resistance leads, and the output and diode gold bonding pads were fabricated using thin-film deposition and photoetching techniques. They reside on a 0.25-mm-thick aluminum-oxide (Al_2O_3) substrate, as shown in Fig. 3.

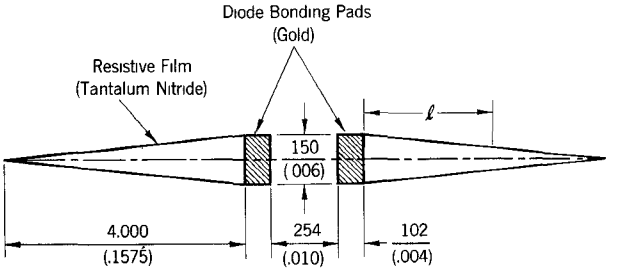

Fig. 1. The 8-mm resistively tapered dipole element. Dimensions are in millimeters (and inches).

B. Detector Diode Selection

Low-barrier, beam-lead Schottky detector diodes were ultrasonically bonded across the dipole gap of each element of the broad-band E-field probe. The particular detector diode used was very carefully selected from the broad range of commercially available beam-lead detector diodes. The predominant diode characteristics used in the diode selection were: 1) maximum operating frequency (F_{max}); 2) diode junction capacitance (C_j); 3) diode junction resistance (R_j), and 4) detection sensitivity. High F_{max} dictates minimum C_j and parasitic reactances such as the package capacitance (C_p) and diode lead inductance (L). It is also important that C_j be very small because it forms a voltage divider with the driving point capacitance (C_a) of the dipole antenna, as shown in the dipole–diode equivalent circuit of Fig. 4. Consequently, only diodes with $C_j \leqslant 0.1$ pF were considered. Since C_a combines with R_j to form a high-pass filter, which, in turn, determines the low-frequency cutoff (f_L), only diodes with relatively large values of R_j were considered. Also, the very wide frequency range (100 kHz to 18 GHz) placed high sensitivity requirements on the detecting diode—especially at the low-frequency limit ($\approx$100 kHz). Consequently, only low-barrier diodes and zero-bias Schottky (ZBS) diodes were initially considered. Actually, there was some concern regarding the loading effect that a ZBS diode might impose on the Z_a of the dipole antenna. However, it was expected that several compromises would have to be made between high R_j, wide frequency coverage, flat frequency response, etc. For example, large values of R_j require large load resistance (R_l), which is usually the input resistance of the readout meter. The larger the values of R_j and R_l, the greater is the tendency for EM field pickup and distortion caused by the high-resistance lines which connect the dipole antenna to the readout device.

Several selected Schottky diode types were further evaluated using a detector test fixture that firmly held a beam-lead diode across the gap of an 8-mm metal dipole. Frequency response measurements of the dipole–diode combinations were made using 1) a TEM cell (12 cm×12 cm), which provided standard fields of 5 and 10 V/m at frequencies up to 1 GHz and 2) a "hooded-horn" configuration that provided standard fields at 6, 8, 10, and 12 GHz. Three of the measured response curves are illustrated in Fig. 5. The rapid increase in response for all three curves, for frequencies above 6 GHz, can be solely

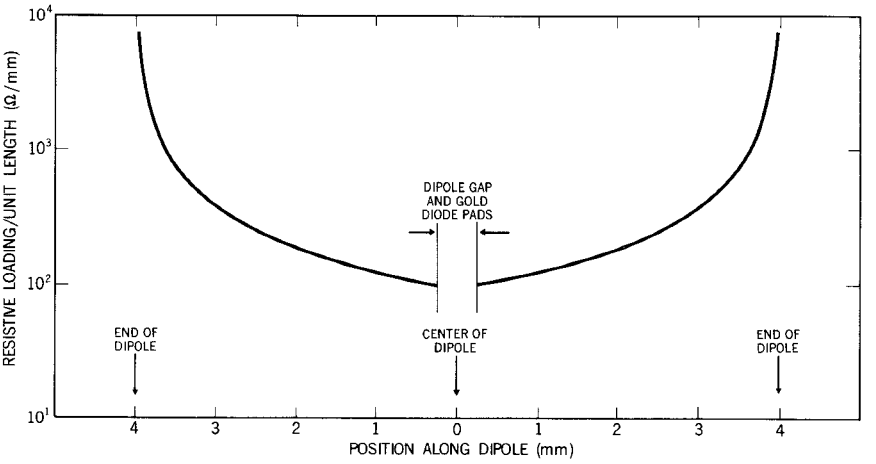

Fig. 2. The resistive tapering profile of the 8-mm dipole.

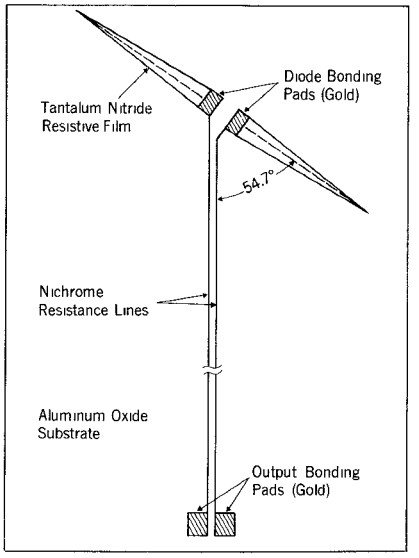

Fig. 3. The 8-mm thin-film dipole antenna composite.

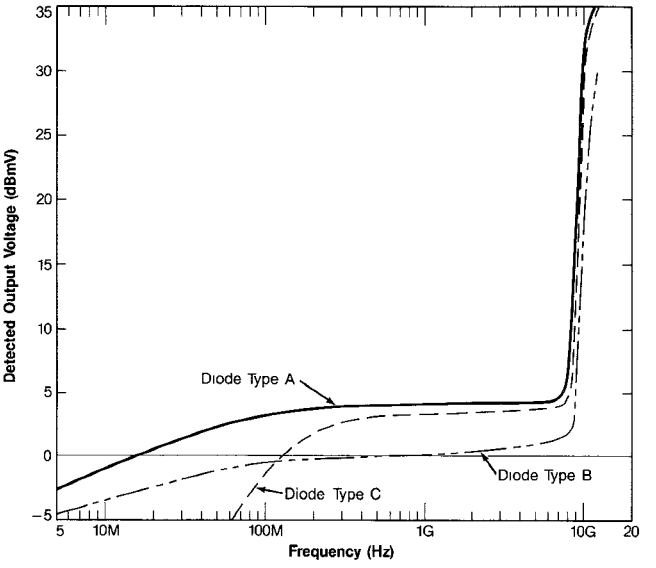

Fig. 5. The frequency responses of three selected diode types, as measured using an 8-mm metal dipole test fixture.

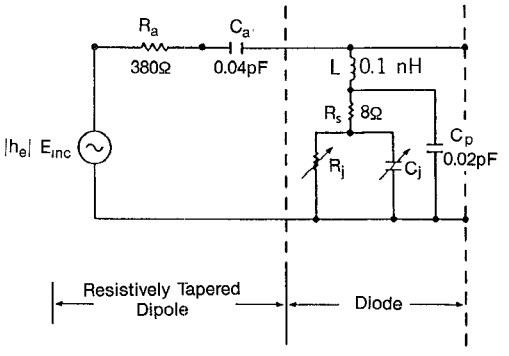

Fig. 4. The dipole–diode equivalent circuit model.

attributed to the resonant frequency of the 8-mm metal dipole. Response differences between the three diode types are quite evident for frequencies below 8 GHz, however. For example, the response curve for the type-C diode has a relatively high f_L. This is not surprising since this is a ZBS diode, and consequently has a relatively low value of R_j at zero bias (5 to 15 kΩ). As previously stated, this R_j combines with C_a to form a high-pass filter; thus, f_L is inversely proportional to its magnitude. In comparison, the response of diode type A has an f_L which is well below 5 MHz. This detector diode is an N-type, low-barrier Schottky diode which has an R_j of between 1 and 2 MΩ. A second low-barrier Schottky diode, type B, also has an f_L which occurs below 5 MHz, but its sensitivity is seen to be 2 to 5 dB lower than that of diode type A over the frequency range of interest. Since diode type A exhibited the greatest sensitivity and yielded a relatively flat response between 10 MHz and 6 GHz, it was selected as the optimum detector for the 8-mm resistive dipole probe.

C. The High-Resistance Thin-Film Transmission Lines

The high-resistance thin-film transmission lines on each dipole substrate create a low-pass distributed filter composed of a highly lossy series inductance with distributed interlead capacitance. They are effectively transparent to RF and microwave fields. These transmission lines were

fabricated by photoetching a thin film or Nichrome (NiCr), which has a surface resistance of 250 Ω/sq. Each line of the pair is 0.025 mm wide, is spaced 0.025 mm from its counterpart, and is approximately 40 mm long. Also, the total resistance of each line is approximately 400 kΩ.

Using the present configuration of the high-resistance, thin-film transmission line, its inductance (L) and capacitance (C) per unit length are given as follows [8]:

$$L = \frac{\mu_0}{\pi}\left[\ln\left(1+\frac{d}{a}\right)+\frac{d}{a}\ln\left(1+\frac{a}{d}\right)\right] \tag{5}$$

and

$$C = \epsilon_0 \frac{\pi}{\left[\ln\left(1+\frac{d}{a}\right)+\frac{d}{a}\left(1+\frac{a}{d}\right)\right]} \tag{6}$$

where a is the width of each conductor of the lossy transmission line, d is the separation between the two conductors, ϵ_r is the relative permittivity of the substrate, and ϵ_0 and μ_0 are the permittivity and permeability of free space, respectively.

The attenuation constant of the high-resistance transmission lines is

$$\alpha \cong \left[\frac{\omega C}{2}\left(\sqrt{R^2+\omega^2L^2}-\omega L\right)\right]^{1/2} \cong \sqrt{\frac{\omega RC}{2}} \tag{7}$$

assuming negligible values of shunt conductance and ω^2LC.

For the high-resistance, thin-film Nichrome (250 Ω/sq) transmission lines, which are 0.025 mm wide, spaced 0.025 mm apart, and deposited on an Al_2O_3 substrate ($\epsilon_r = 8$), the typical inductance and the capacitance are $L = 5.55\times 10^{-7}$ H/m and $C = 9.02\times 10^{-11}$ F/m. For the 40-mm-long transmission line with a total resistance of 400 kΩ, the total inductance (L), the total capacitance (C), and the total attenuation (A) are $L = 2.22\times 10^{-8}$ H, $C = 3.61\times 10^{-12}$ F, and $A = 0.67$ Np (at 100 kHz).

III. Theoretical Analyses for the Resistively Tapered Dipole with a Diode Detector Load

Having previously described the impedance profile for the 8-mm resistively tapered dipole with (4), the current distribution along the dipole's length can be calculated. The effective length (h_e) and the driving impedance ($R_a - j1/\omega C_a$) of the antenna are determined from its current distribution

$$h_e = \frac{2}{k^2h}\left(1-jkh-e^{-jkh}\right) \tag{8}$$

and

$$R_a - j\frac{1}{\omega C_a} = 60\psi\left(1-\frac{j}{kh}\right) \tag{9}$$

where the term ψ is previously defined in (3).

The Thévenin's equivalent circuit model for the resistively tapered dipole loaded with a diode detector is shown in Fig. 4. The diode I–V characteristic is given as

$$i = i_s\left(e^{\alpha v}-1\right) \tag{10}$$

where $i_s = 2\times 10^{-9}$ A, and $\alpha = 38$ V^{-1}. The nonlinear diode junction capacitance (C_j) is given as

$$C_j(V) = \frac{C_j(0)}{(1-V/V_b)^{1/2}} \tag{11}$$

where $C_j(0) = 0.10$ pF and $V_b = 0.45$ V. The frequency response of the antenna is determined by analyzing the nonlinear circuit model using the Newton–Raphson iteration method. A detailed discussion is given in a recent paper [9]. Fig. 6 shows the theoretically predicted frequency response of the antenna, based on this theoretical model. Fig. 7 shows the measured dynamic range of the broad-band E-field probe. The detected voltage for electric-field strengths up to approximately 20 V/m has an accurate square-law response which is proportional to E squared. For electric-field strengths above 20 V/m, the detected dc voltage departs from square law, approaching a linear response at approximately 500 V/m. This phenomenon can be relatively easily predicted by solving a first-order differential equation associated with the simplified Thévenin's equivalent nonlinear circuit shown in Fig. 8. It can be shown [3] that for a small induced voltage (V_i), the

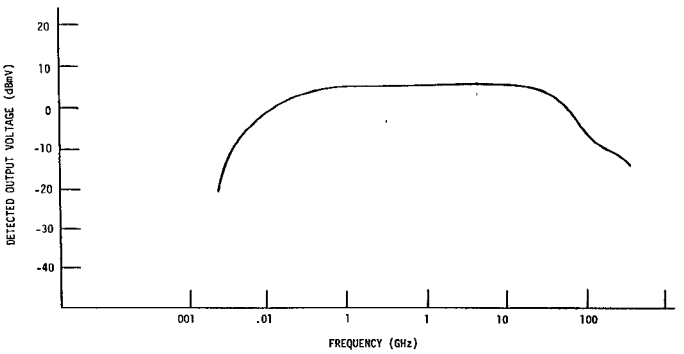

Fig. 6. The theoretically predicted response of the 8-mm resistively tapered dipole antenna.

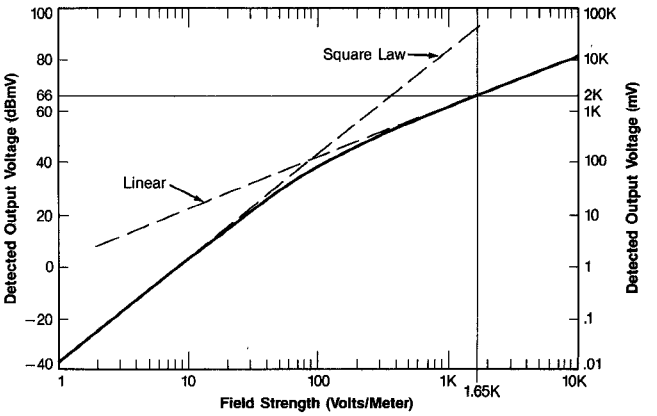

Fig. 7. The measured dynamic range of the 8-mm resistive dipole–diode sensing element.

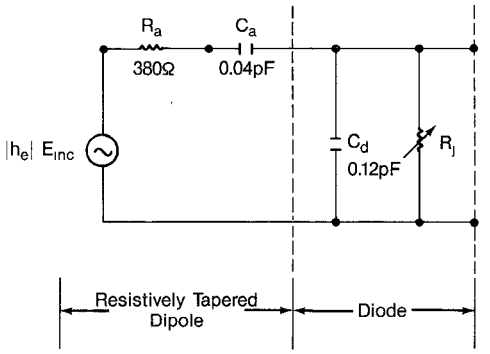

Fig. 8. A simplified equivalent circuit model for the 8-mm resistive dipole–diode sensing element.

output dc voltage (V_0) is

$$V_0 \cong -\frac{\alpha}{4}\left(\frac{V_t}{1+C_d/C_a}\right)^2 \tag{12}$$

and for large V_t

$$V_0 \cong -\frac{V_t}{1+C_d/C_a}. \tag{13}$$

Equation (12) indicates that for small induced RF voltages, the output dc voltage is a square-law function of the induced voltage. On the other hand, (13) indicates that for large induced voltages, the output dc voltage V_0 is directly proportional to the induced voltage. The measured linear, transition, and square-law regions of the detected output voltage can be seen by examination of Fig. 7.

IV. Evaluation of the Broad-Band Electric-Field Probe

The broad-band electric-field probe prototype, configured of resistively tapered dipoles, was calibrated with respect to the following parameters: 1) frequency response, 2) dynamic range, and 3) probe isotropy, that is, antenna directivity and field polarization sensitivity.

The approach used at NBS for evaluating and calibrating RF radiation monitors is to generate a calculable or "standard" field and then immerse the probe of the monitor being tested in this known field. The optimum type of field-generating instrumentation depends on the frequency band and the desired accuracy. A convenient device for frequencies up to 300 MHz is a rectangular "coaxial" transmission line known as a TEM cell. In the frequency range of 300–1000 MHz, a series of rectangular waveguide transmission lines (open-ended waveguides) can be used, in the NBS anechoic chamber, to generate fields of known intensity. Calibration fields above 500 MHz are produced in the NBS anechoic chamber using a series of standard-gain pyramidal horns. In all cases, it is possible to calculate the electric- and magnetic-field strengths (and equivalent free-space power densities) in terms of the measured power flow through the cell or waveguide, or the power delivered to the open-ended waveguide or horn antenna. Such standard fields can be established at NBS at any

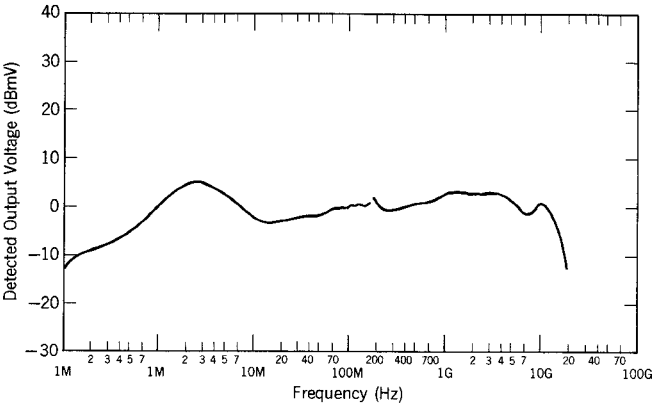

Fig. 9. The measured frequency response of one element of the broad-band E-field probe at 10 V/m.

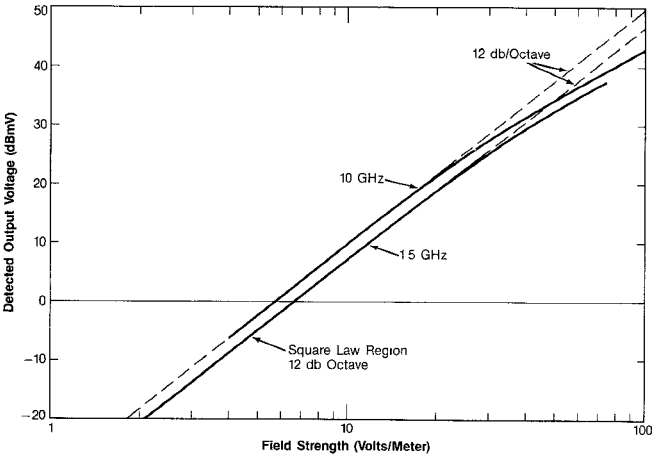

Fig. 10. The measured linearity of the E-field probe at both 1.5 GHz and 10 GHz.

frequency up to 18 GHz with an uncertainty of less than ±1.0 dB.

Fig. 9 shows one dipole's dc output voltages as measured in a standard field of 10 V/m from 100 kHz to 18 GHz. These detected dc voltages were measured using a dc digital voltmeter having an input impedance of 50 MΩ. The probe's response is seen to drop sharply below 1 MHz and beyond 12 GHz. Fig. 7 shows the measured plus projected dynamic range of the prototype E-field probe. As discussed in Section III, the detected dc voltage has an accurate square-law response for electric fields of less than 20 V/m. When the electric-field strength is above 20 V/m, however, the detected dc voltage departs from square law, approaching a linear response near 500 V/m. Since the Schottky beam-lead diode used has a breakdown voltage of about 4 V, the expected maximum electric field that the probe can measure (without damage) is estimated to be about 1.65 kV/m. The minimum measurable field strength is about 1 V/m when conventional measurement systems are used. Since this sensitivity is system-noise-dependent, it should be possible to improve this value by at least an order of magnitude by using a synchronous detection scheme in applications in which the EM field can be amplitude modulated. Probe linearity is very weakly dependent on frequency, as indicated in the curves of Fig. 10.

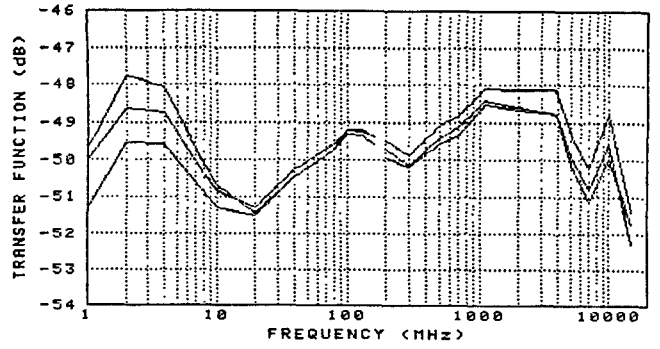

Fig. 11. The individual transfer function of all three sensing elements of the probe at 10 V/m.

Since the broad-band electric-field probe was calibrated at 10 V/m, where the detected voltage has a square-law response, it is appropriate to define the transfer function of the probe, in dB, as

$$T_{\mathrm{dB}} = 10 \log \frac{V_{\max}}{E_{\mathrm{inc}}^2} \tag{14}$$

where $V_{\max}$ is the maximum dc detected voltage and E_{inc} is the incident electric-field strength. Fig. 11 shows the measured transfer functions of each element of the broad-band electric-field probe, which are flat to within ± 2 dB from 1 MHz to 15 GHz.

Probe isotropy is achieved by the mutually orthogonal configuration of the three dipole elements, and its measure can be obtained by correctly combining the three dc detected output voltages. When the probe is operated in its square-law region, i.e., the dc detected output voltages are proportional to the corresponding electric-field components squared, the magnitude of the electric-field strength can be defined as

$$|E| = k\left(V_x + V_y + V_z\right)^{1/2} \tag{15}$$

where k is a constant of proportionality and the V's are the three detected output voltages. It is important to note that (15) is a special case of the more general expression

$$|E| = \left(|E_x|^2 + |E_y|^2 + |E_z|^2\right)^{1/2} \tag{16}$$

where the E's are the electric-field-strength components. Equation (15) can only be used when $|E| \leqslant 20$ V/m. For field strengths greater than 20 V/m, the quantities V_x, V_y, and V_z must be appropriately combined using computer calibration processing or by some form of electronic signal processing afforded by the metering unit. The reception patterns and probe isotropy, illustrated in Figs. 12 and 13, were obtained by aligning the axis of the probe handle such that it made equal angles with the E-vector, the H-vector, and the Poynting vector of a 10-V/m EM field. Measurements were then made and recorded of each dipole's output voltage as the probe was rotated through 360° about the handle's longitudinal axis. The isotropic trace was then computer calculated using (15). It is important to emphasize here that the curves of Figs. 12 and 13 are correct for the probe alignment described and may not represent results obtained using other orientations and/or axes of rotation.

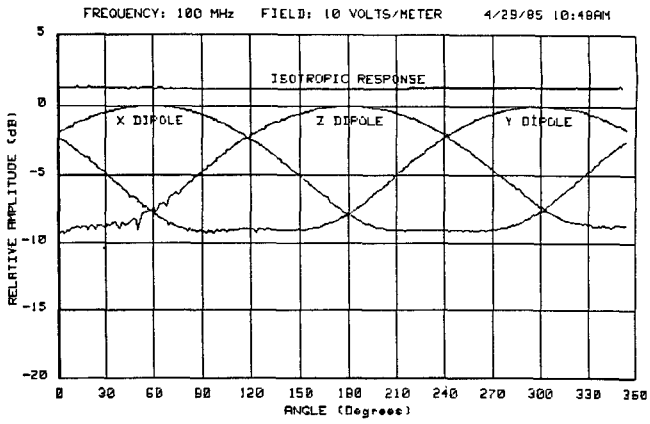

Fig. 12. The reception characteristics of the isotropic E-field probe at 100 MHz.

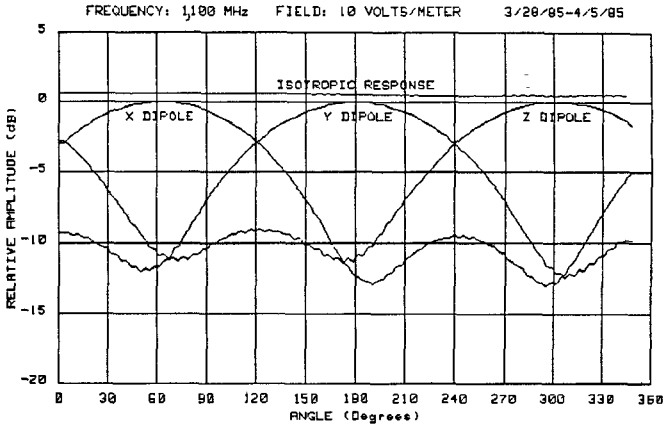

Fig. 13. The reception characteristics of the isotropic E-field probe at 10 GHz.

V. Conclusions

This paper has discussed the essential role that the transfer-standard probe plays in establishing and characterizing standard EM fields. More importantly, it has focused on the theoretical and experimental developmental aspects required to produce and certify a transfer-standard probe. The use of resistive tapering, by means of thin-film deposition and photoetching techniques, has been shown to yield significant improvements over conventional dipole elements. These include broader bandwidth, flatter frequency response, wider dynamic range, smaller size, reduced EM-field perturbation and distortion, and complete absence of in-band resonances.

The use of high-frequency Schottky beam-lead diodes allows the prototype broad-band E-field probe to sense fields of 1 to 1600 V/m over a range of 100 kHz to 18 GHz. Square-law response (dc detected output voltage proportional to the electric field squared) for these detectors covers a range of 1 to 20 V/m. Beyond 20 V/m, the response enters a transition zone (between square law and linear) and becomes linear for field strengths of 500 V/m and above. The minimum field strength that can be measured by the probe is approximately 1 V/m, which is

primarily dictated by measurement system noise. The predicted maximum E-field that the probe can measure, without exceeding the 4-V diode breakdown voltage, is about 1.65 kV/m. The mutually orthogonal configuration of the probe's three sensing elements yields a nearly ideal isotropic response (within ± 0.3 dB).

The broad-band isotropic E-field probe was originally designed to serve as a transfer-standard in establishing, maintaining, and certifying controlled EM environments in the laboratory. Since its development, however, considerable interest has come from other applications which require precise EM characterization of complex fields in the near-zones of highly sensitive electronic systems and components. The miniature probe size should allow high spatial resolution in such applications. There is also interest in using arrays of this probe for periodic certification of such testing facilities as anechoic chambers, reverberation chambers, and open-field ranges. And finally, some consideration is being given to appropriate modifications to the probe which would extend its utility to include the measurement of very large impulse fields.

References

[1] M. Kanda, "A methodology for evaluating microwave anechoic chamber measurements," in *Proc. EMC Symp.*, Mar. 5–7, 1985.

[2] N. S. Nahman, M. Kanda, E. B. Larsen, and M. L. Crawford, "Methodology for standard electromagnetic field measurements," *IEEE Trans. Instrum. Meas.*, vol. IM-24, no. 4, pp. 490–503, Dec. 1985.

[3] M. Kanda, "Analytical and numerical techniques for analyzing an electrically short dipole with a nonlinear load," *IEEE Trans. Antennas Propag.*, vol. AP-28, no. 1, Jan. 1980.

[4] E. B. Larsen and F. X. Ries, "Design and calibration of the NBS isotropic electric-field monitor [EFM-5], 0.2 to 1000 MHz," *Nat. Bur. Stand. (U.S.) Tech Note 1033*, Mar. 1981.

[5] G. S. Smith, "Limitations on the size of miniature electric-field probes," *IEEE Trans. Microwave Theory Tech.*, vol. MTT-32, no. 6, June 1984.

[6] M. Kanda, "A relatively short cylindrical broad-band antenna with tapered resistive loading for picosecond pulse measurements," *IEEE Trans. Antennas Propag.*, vol. AP-26, no. 3, May 1978.

[7] T. T. Wu and R. W. P. King, "The cylindrical antenna with nonreflecting resistive loading," *IEEE Trans. Antennas Propag.*, vol. AP-13, no. 3, pp. 369–373, May 1965.

[8] M. Kanda, L. Driver, and D. Melquist, "Development of a broad-band, isotropic electric-field probe using resistively tapered dipole antennas, 100 kHz to 18 GHz," *Nat. Bur. Stands. (U.S.) Tech. Note*, in preparation.

[9] M. Kanda, "The time-domain characteristics of a traveling-wave linear antenna with linear and nonlinear parallel loads," *IEEE Trans. Antennas Propag.*, vol. AP-28, no. 2, Mar. 1980.

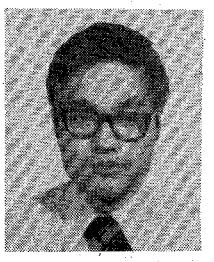

Motohisa Kanda (S'67–M'68–SM'83) received the B.S. degree from Keio University, Tokyo, Japan, in 1966, and the M.S. and Ph.D. degrees in electrical engineering from the University of Colorado, Boulder, in 1968 and 1971, respectively.

From 1965 to 1966, he did research on the avalanche breakdown in germanium p-n junctions at cryogenic temperatures at Keio University. From 1966 to 1971, he was a Research Assistant at the University of Colorado, where he was engaged in research on the impact ionization of impurities in n-type germanium and on nonreciprocal behavior in solid-state magnetoplasma at millimeter and submillimeter wavelengths. In 1971, he joined the National Bureau of Standards, Boulder, CO, where he is presently group leader of the Fields Characterization Group of the Electromagnetic Fields Division. Concurrently, he has been a professor adjoint in the Electrical Engineering Department of the University of Colorado, Boulder.

Dr. Kanda is a full member of Sigma Xi and of Commissions A, B, and E of the International Union of Radio Science.

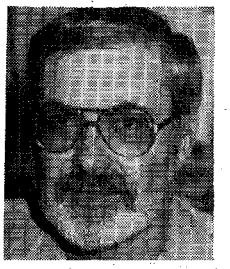

Lanny D. Driver received the B.S.E.E. degree from the University of Kansas in 1961.

After almost a year at KU's Electronics Research laboratory, he joined the Boulder Laboratories of NBS. From 1962 to 1980, he worked in RF noise metrology and in developing RF noise standards, RF noise radiometers, and noise metrology techniques. In 1980, he joined the Fields Characterization Group of the Electromagnetic Fields Division, and has since been heavily involved in the development of various types of EM field probes, sensors, and antennas.